

Article

Cartilage Differentiation of Bone Marrow-Derived Mesenchymal Stem Cells in Three-Dimensional Silica Nonwoven Fabrics

Shohei Ishikawa ¹, Kazutoshi Iijima ^{2,†}, Kohei Sasaki ³, Mineo Hashizume ², Masaaki Kawabe ³ and Hidenori Otsuka ^{1,4,*} 

¹ Graduate School of Science, Tokyo University of Science, 1-3 Kagurazaka, Shinjuku-ku, Tokyo 162-8601, Japan; 1317703@ed.tus.ac.jp

² Department of Industrial Chemistry, Faculty of Engineering, Tokyo University of Science, 12-1 Ichigayafunagawara-machi, Shinjuku-ku, Tokyo 162-0826, Japan; iijima-kazutoshi-mh@ynu.ac.jp (K.I.); mhashizu@ci.kagu.tus.ac.jp (M.H.)

³ Japan Vilene Company Ltd., 7 kita-Tone, Koga, Ibaraki 306-0213, Japan; kh-sasaki@vilene.co.jp (K.S.); m-kawabe@vilene.co.jp (M.K.)

⁴ Department of Applied Chemistry, Faculty of Science, Tokyo University of Science, 1-3 Kagurazaka, Shinjuku-ku, Tokyo 162-8601, Japan

* Correspondence: h.otsuka@rs.kagu.tus.ac.jp; Tel.: +81-3-5228-8265

† Present address: Faculty of Engineering, Yokohama National University, 79-5 Tokiwadai, Hodogaya-ku, Yokohama 240-8501, Japan.

Received: 24 June 2018; Accepted: 16 August 2018; Published: 18 August 2018



Featured Application: Silica nonwoven fabrics are materials with mechanical strength and cellular functions for potential cartilage regeneration applications.

Abstract: In cartilage tissue engineering, three-dimensional (3D) scaffolds provide native extracellular matrix (ECM) environments that induce tissue ingrowth and ECM deposition for in vitro and in vivo tissue regeneration. In this report, we investigated 3D silica nonwoven fabrics (Cellbed[®]) as a scaffold for mesenchymal stem cells (MSCs) in cartilage tissue engineering applications. The unique, highly porous microstructure of 3D silica fabrics allows for immediate cell infiltration for tissue repair and orientation of cell–cell interaction. It is expected that the morphological similarity of silica fibers to that of fibrillar ECM contributes to the functionalization of cells. Human bone marrow-derived MSCs were cultured in 3D silica fabrics, and chondrogenic differentiation was induced by culture in chondrogenic differentiation medium. The characteristics of chondrogenic differentiation including cellular growth, ECM deposition of glycosaminoglycan and collagen, and gene expression were evaluated. Because of the highly interconnected network structure, stiffness, and permeability of the 3D silica fabrics, the level of chondrogenesis observed in MSCs seeded within was comparable to that observed in MSCs maintained on atelocollagen gels, which are widely used to study the chondrogenesis of MSCs in vitro and in vivo. These results indicated that 3D silica nonwoven fabrics are a promising scaffold for the regeneration of articular cartilage defects using MSCs, showing the particular importance of high elasticity.

Keywords: cartilage tissue engineering; mesenchymal stem cells; 3D scaffold; electrospun nanofiber; silica nonwoven fabrics

1. Introduction

Articular cartilage is hyaline cartilage covering the articular surface of bones. Because of its avascular characteristic, once injured, articular cartilage has poor self-repair abilities. The management

of injured cartilage involves conservative and surgical approaches, but there is currently no effective treatment. Bone marrow stimulation (microfracture surgery) could induce cartilage formation, but the newly formed cartilage is fibrocartilage instead of hyaline cartilage [1–3]. Several methods of chondrocyte implantation have been used to treat cartilage defects in humans, but implanted grafts do not provide mechanical stability, and various side effects lead to procedure failure [4,5]. Osteochondral plug transplantation (mosaicplasty) has been developed, but the limitations of this technique include donor site morbidity and the limited availability of grafts that can be harvested [6,7]. The long-term outcome is constrained by the age and gender of the patient and the size of the wound [6].

Recently, mesenchymal stem cells (MSCs) have received much attention as a cell source for cartilage cell therapy [8–10]. MSCs isolated from bone marrow and adipose tissue have the ability to differentiate into various types of cells in mesodermal lineages, such as osteoblasts, chondrocytes, adipocytes, myocytes, and cardiomyocytes [11–13].

For efficient cartilage tissue formation of MSCs, a variety of scaffolds providing structural support to MSCs and facilitating their chondrogenic differentiation to form three-dimensional (3D) cartilage-like tissue are needed. MSC-seeded scaffolds for cartilage tissue regeneration should be biocompatible and biodegradable. Biopolymers and polymers used as these scaffolds have been reviewed in terms of state of the art and future trends. Furthermore, to fabricate a uniform cellular matrix, scaffold porosity should be high to provide sufficient space for extracellular matrix (ECM) regeneration, and the pore structure should be interconnected so that spatially homogeneous tissue formation can occur [14].

Approaches using 3D scaffolds and MSCs to remodel cartilage have resulted in the development of strategic natural biomaterials such as scaffolds based on agarose, chitosan, hyaluronic acid, and collagen [14,15]. Collagen has recently been explored in numerous applications in tissue engineering and regenerative medicine. Atelocollagen has been investigated largely because of its antigenic determination on the peptide chains and its ability to manipulate the backbone of amino residues [16]. Atelocollagen is clinically used as an artificial substitute in plastic surgery and dermatology, but its shrinking property, lower elasticity, and inflammatory response are major concerns for the formation of ECM-like structures at defect sites [17]. Moreover, since highly rigid scaffolds compatible with native cartilage tissue (10–20 MPa) are desirable in cartilage tissue regeneration using MSCs [18], atelocollagen gels are not suitable for this application. Thus, the development of scaffold-like silica nonwoven fabrics that replace atelocollagen gels has been demanded.

Furthermore, 3D cell culture systems mimicking *in vivo* environments have been developed to control MSC differentiation. In tissue engineering for regenerative medicine and *in vitro* assay technology, 3D cell culture systems provide higher cellular functionality than traditional two-dimensional (2D) cell culture. There are various 3D cell culture methods, including spheroid formation [19,20] and cell seeding in scaffolds, such as polymer hydrogels [21,22], porous materials [23,24], and fibrous fabrics [25]. Recently, 3D printing of cell constructs has received much attention as a low-cost technique to fabricate cellular scaffolds that possess high mechanical strength and enable enhanced cellular performance [26]. This technique has the potential to create implant matrix substitutes to articular tissue. However, the fabrication of scaffolds with microscopic structures and low porosity (<50%) is challenging [26].

Among scaffolds, fibrous fabrics prepared by electrospinning techniques show excellent properties because their structural morphologies are similar to those of fibrillar ECM. Nonwoven nanofibrous scaffolds are mainly fabricated by biocompatible polymers such as polycaprolactone [27], poly(ethylene terephthalate) [28], poly-L-lactide [29], polyethersulfone [30], and their derivatives. They provide excellent culture advantages, such as high surface area-volume capacity, by reducing the physical interaction and enhancing the mechanical strength. These nanostructured fibrous fabrics can be utilized for cell therapy to regulate drug and cell factors after transplantation. Furthermore, their native-like ECM morphology induces cell-ECM interactions, promotes active cell signaling pathways, and supports stem cell differentiation.

In this study, we investigated 3D silica nonwoven fabrics (Cellbed[®]) as a scaffold for MSCs in cartilage tissue engineering applications. Highly porous 3D silica nonwoven fabrics with interconnected

microstructures were developed by electrospinning through the sol-gel process. The random orientation of the silica fibers produces many interconnected pores that may promote cellular migration and tissue ingrowth and prevent shrinkage because of the sufficient mechanical strength of the fabrics [31,32]. As a result of these characteristics, fibroblasts migrated into and penetrated the 3D silica fabrics and showed remarkable growth rates compared with those in traditional 2D culture [33–35]. Moreover, the functions of hepatocytes co-cultured with fibroblasts in 3D silica fabrics were significantly enhanced compared with those of 2D fibroblasts because of the abundance of fibroblast-secreted soluble factors, which are important for maintaining hepatocytes [35]. We have recently demonstrated that osteogenic differentiation was significantly promoted in 3D silica fabrics.

Silica-based hybrid materials have been widely used as implantable materials for cartilage and bone tissue regeneration. For example, Kascholke et al. developed biodegradable and adjustable sol-gel glass-based hybrid scaffolds for cartilage and bone tissue regeneration [36]. This scaffold was biodegradable, and MSCs embedded in the scaffold proliferated and displayed promoted cell function. However, this scaffold lacks molding properties, and its porosity and shrinking property are limitations. Thus, 3D silica nonwoven fabrics are useful as scaffolds for cartilage tissue regeneration because of their easy molding, ECM-like network structure, high mechanical strength, and porosity.

2. Materials and Methods

2.1. Materials

Silica nonwoven fabrics compatible with 12-well culture inserts (Cellbed[®], porosity as high as >95%, mean flow pore diameter of 7.6 μm , diameter of 10 mm, and thickness of 182 μm) were kindly supplied by Japan Vilene Co. Ltd. (Ibaraki, Japan). Atelocollagen (3%) was obtained from KOKEN (Tokyo, Japan). All chemicals were purchased from Wako Pure Chemicals, Inc. (Osaka, Japan) and used without further purification. Culture-treated 12-well polystyrene plates were obtained from Becton, Dickinson and Co. (Franklin Lakes, NJ, USA).

2.2. Cell Culture

Human bone marrow-derived MSCs with an extended lifespan through retroviral transduction (UE7T-13 cells) were obtained from the Japanese Collection of Research Bioresources Cell Bank, National Institute of Biomedical Innovation (Tokyo, Japan). UE7T-13 cells [37] were maintained in standard Dulbecco's modified Eagle's medium (D-MEM, Life Technologies Corp., Carlsbad, CA, USA) supplemented with 10% (vol./vol.) fetal bovine serum (FBS, SAFC Biosciences, Inc., Lenexa, KS, USA), 100 U/mL penicillin, and 100 mg/mL streptomycin (Sigma-Aldrich Japan Corp., Tokyo, Japan) (hereafter denoted as D-MEM(+)) at 37 °C in a humidified 5% CO₂ atmosphere.

2.3. Preparation of Silica Nonwoven Fabrics

Tetraethoxysilane as a metal compound, ethanol as a solvent, water for hydrolysis, and 1 N hydrochloric acid as a catalyst were mixed at a molar ratio of 1:5:2:0.003 and refluxed at 78 °C for 10 h. The solvent was then removed, and the mixture was heated to form a sol solution. By using the resulting sol solution as a spinning solution, gel silica fiber webs were prepared according to a plate spinning technique, which is an electrospinning method.

2.4. Induction of Chondrogenic Differentiation of MSCs

MSCs (3×10^5) dispersed in 500 mL of D-MEM(+) were seeded on 3D silica fabrics in 12-well culture inserts (Becton, Dickinson and Co., Franklin Lakes, NJ, USA) and precultured for 1 week. Then, the cell culture medium was replaced with chondrogenic differentiation medium (PromoCell, GmbH, Heidelberg, Germany). As a control experiment, 0.5% atelocollagen gels were prepared by diluting the original 3% atelocollagen gel with normal medium. Hydrogelation was performed in a 1.5 mL sampling tube, and 50 μL of hydrogel containing cells at a density of 1×10^7 cells/mL

was incubated at 37 °C for 3 h and then cultured with normal medium. The encapsulated cells were precultured for three days, and the cell culture medium was changed to chondrogenic differentiation medium. In addition, spheroid culture was performed in a 96-well U-bottom cell culture plate. MSCs (1.0×10^5) dispersed in 100 μ L of normal medium were seeded in each well of a 96-well U-bottom plate and precultured for 3 days. The cell culture medium was then replaced with chondrogenic differentiation medium. Media were changed every 3 days and cells were further cultured for 4 weeks.

2.5. Confocal-Laser Scanning Microscopic (CLSM) Observation

Cells (3×10^5) dispersed in 500 μ L of D-MEM(+) were seeded on 3D silica fabrics in 12-well culture inserts and cultured at 37 °C and precultured for 1 week. Then, the cell culture medium was replaced with chondrogenic differentiation medium, and the medium was changed every 3 days. After 2 weeks and 4 weeks of culture, CLSM (LSM-710, Carl Zeiss Co, Ltd., Oberkochen, Germany) images were obtained. Cells were treated with 5 mg/mL Hoechst 33342 (Dojindo laboratories, Kumamoto, Japan) in D-MEM(+) for 1 h in the dark. Then, the cells were washed three times with phosphate-buffered saline (PBS) and fixed with 4 wt% paraformaldehyde solution in PBS for 20 min followed by permeation with 0.5% Triton X-100 solution for 2 min. Cells were treated with 1% Alexa Fluor 594 phalloidin (Life Technologies, Corp., Carlsbad, CA, USA) for 2 h. After washing with PBS three times, cells were observed by CLSM.

2.6. Cell Number Analysis

After 4 weeks of culture, cells in 3D silica fabrics were evaluated using a hemocytometer. Briefly, the 3D silica fabrics were exposed in 0.5% trypsin-EDTA for 5 min, pipetted for some time, and washed with PBS. The trypsinized solution was collected, and cell number was counted using a hemocytometer. Data are shown as mean \pm standard error of the mean of triplicates.

2.7. Quantification of Glycosaminoglycan and Collagen Content

The production of sulfate glycosaminoglycan (GAG) was determined by the modified dimethyl-methylene blue (DMMB) method [38]. The cultured sample was washed three times with PBS and digested individually in 2 N NaOH at 60 °C for 24 h. The digested sample was stored at -20 °C until further analysis. To determine GAG content, the digested sample was assayed by DMMB dye, and the absorbance was monitored at 570 nm with a microplate reader. The GAG content was extrapolated from a standard curve using shark chondroitin sulfate (Sigma-Aldrich Japan Co., Tokyo, Japan). Three parallels were averaged for each specimen.

Total collagen content was estimated by measuring the hydroxyproline content according to a previous report [39]. The collected sample was hydrolyzed in 5 N HCl at 110 °C for 24 h. The hydroxyproline content of hydrolysate was determined using chloramine-T/Ehrlich's reagent assay, and the color change was quantified spectrophotometrically at 560 nm. The standard curve was generated with l-hydroxyproline, and a conversion factor of 10 was used to convert from hydroxyproline to total collagen content [40].

2.8. Real-time Reverse-Transcription Polymerase Chain Reaction (qRT-PCR)

Total RNA was extracted from cultured cells with an RNeasy[®] mini kit (Qiagen, Inc., Hilden, Germany) combined with Trizol[®] (Thermo Fisher Scientific Inc., Waltham, MA, USA). Briefly, cells were dispersed and homogenized in Trizol[®] using Powermasher (Nippi, Inc., Tokyo, Japan) and Biomasher II (Nippi, Inc., Tokyo, Japan), and total RNA was extracted according to the manufacturer's instructions. cDNA was generated with a ReverTra Ace[®] qPCR RT Master Mix with a gDNA Remover (Toyobo Co., Ltd., Osaka, Japan) according to the manufacturer's instructions. qRT-PCR was performed using the Thunderbird[®] SYBR[®] qPCR Mix (Toyobo Co., Ltd., Osaka, Japan) on an ABI PRISM 7900HT Sequence Detection System (Applied Biosystems, Inc., Foster City, CA, USA). The relative quantification was calculated via the $\Delta\Delta$ Ct method and normalized against the housekeeping *GAPDH*. The following

primers were used: *COL1A1* (5'-gtcgaggccaagacaag-3' (sense) and 5'-cagatcacgtcatcgacaac-3' (antisense)) [41], *COL2A1* (5'-ggcaatagcaggttcacgtaca-3' (sense) and 5'-cgataacagtcttgcccactta-3' (antisense)) [42], *COL10A1* (5'-gtctgcttttactgttattctctcaaa-3' (sense) and 5'-tgctgttgctgttatacaaaattt-3' (antisense)) [43], *ACAN* (5'-agcctgcgctccaatgact-3' (sense) and 5'-taatggaacacgatgccttca-3' (antisense)) [44], *SOX9* (5'-ttccgcagctggacat-3' (sense) and 5'-tcaaactcgttgacatcgaaggt-3' (antisense)) [45], and *GAPDH* (5'-agcaagagcacaagaggaagaga-3' (sense) and 5'-gaggggagattcagtgtggtg-3' (antisense)).

3. Results

3.1. Proliferation and Morphology of Chondrogenic MSCs Cultured in 3D Silica Fabrics

The proliferation and morphology of chondrogenic-differentiated MSCs cultured in 3D silica fabrics were observed using CLSM (Figure 1). CLSM images of MSCs in silica fabrics cultured with normal medium (Diff (–)) and chondrogenic differentiation medium (Diff (+)) after 2 weeks and 4 weeks in culture are shown in Figure 1. After 2 weeks of culture, MSCs were detected at a depth of approximately 48 μm under both culture conditions, and no difference was observed in terms of MSC morphology. After 4 weeks of culture, differentiated MSCs but not normal MSCs were detected at a depth of approximately 73 μm . Moreover, normal MSCs were crowded on the 3D silica fabric surface. These results suggested that differentiated cells cultured in Diff (+) preferentially migrated vertically in 3D silica fabrics without proliferation. These proliferation results are related to cell number.

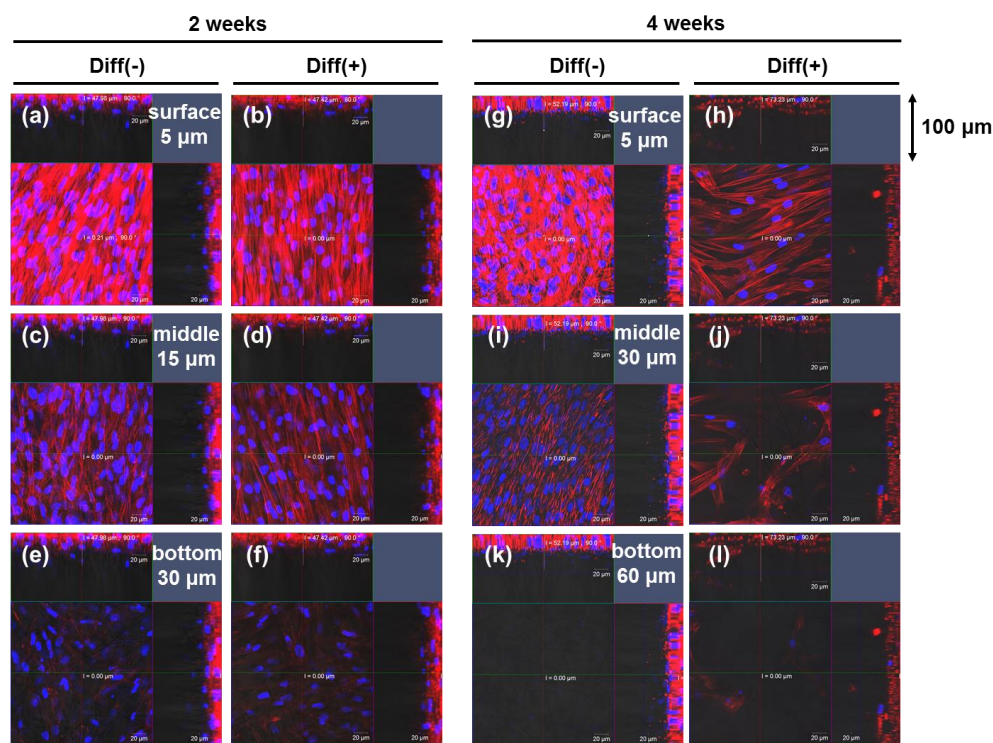


Figure 1. Confocal-laser scanning microscopic (CLSM) images showing proliferation and morphology of mesenchymal stem cells (MSCs) cultured in normal medium (Diff (–)) and chondrogenic differentiation medium (Diff (+)) on three-dimensional (3D) silica nonwoven fabrics for 2 weeks (a–f) and 4 weeks (g–l). In each case, single optical slices near the surface (5.0 μm : a, b, g, h), in the middle (15 μm : c, d, 30 μm : i, j), and near the bottom (30 μm : e, f, 60 μm : k, l) of the silica fabrics are shown. Cellular nuclei and skeletons were stained with Hoechst 33342 (blue) and Alexa Fluor 594 phalloidin (red), respectively. Scale bars: 20 μm .

Figure 2 shows the number of cells adhered to the 3D silica fabrics under normal and differentiation conditions after 4 weeks of culture. The number of adhered cells in the 3D silica fabrics under differentiation condition was controlled compared with that in normal condition.

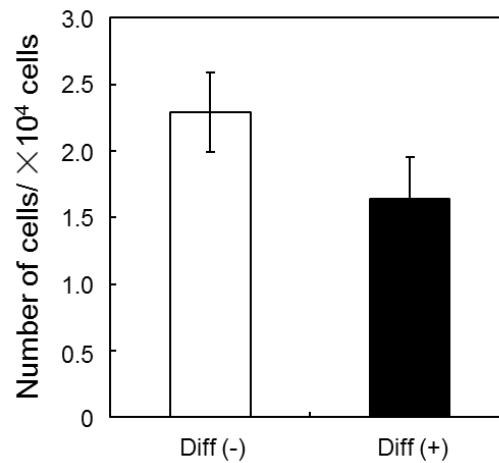


Figure 2. Number of cells in 3D silica fibers cultured in normal medium (Diff (-)) and chondrogenic differentiation medium (Diff (+)) for 4 weeks after seeding at a density of 3.0×10^5 cells/well and preculturing for 1 week.

3.2. Quantification of GAG and Collagen Content

To evaluate the biochemical functionality of these scaffolds, chondrogenic differentiation behavior was investigated in terms of the accumulation of glycosaminoglycan (GAG) and collagen (COL) in the scaffold. Atelocollagen gels and spheroids cultured in 96-well plates, which are commodity scaffolds, were used as controls. Figure 3 shows the accumulation of GAG after 4 weeks of culture in atelocollagen gels, spheroids, and 3D silica fabrics under normal and differentiation conditions. GAG is one of the chondrogenic factors in cartilages. In spite of cultivation in both atelocollagen gel and spheroid culture under normal and differentiation conditions, no difference in accumulation was observed in either condition. Although accumulation in the 3D silica fabrics was inferior to those in the other scaffolds, accumulation under differentiation condition was significantly superior to that under normal condition.

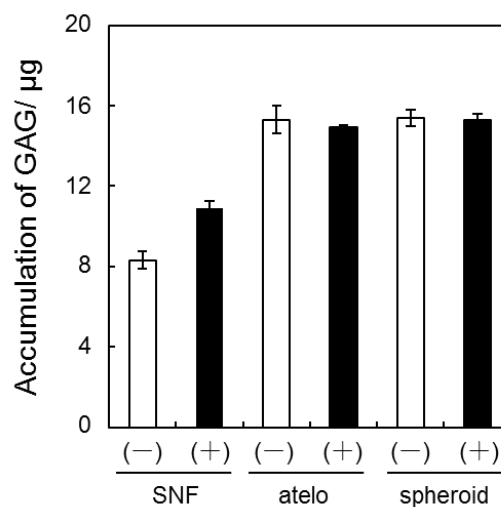


Figure 3. Accumulation of glycosaminoglycan (GAG) in normal medium (Diff (-)) and chondrogenic differentiation medium (Diff (+)) on 3D silica fibers, atelocollagen gels, and spheroids for 4 weeks.

Figure 4 shows the accumulation of COL after 4 weeks of culture in 3D silica fabrics, atelocollagen gels, and spheroids under normal and differentiation conditions. Here, because atelocollagen itself was detected by the hydroxyproline assay, COL accumulation could not be accurately quantified. The accumulation of COL under differentiation condition was superior to that under normal condition in both spheroid and 3D silica fabric culture. However, COL accumulation in 3D silica fabrics was inferior to that in spheroid culture under differentiation condition.

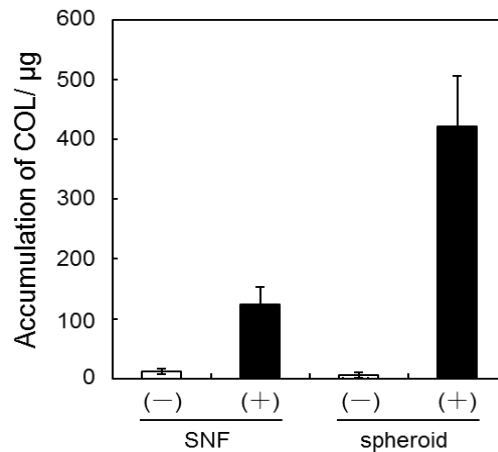


Figure 4. Accumulation of collagen (COL) in MSCs on 3D silica fibers and spheroids cultured in normal medium (Diff (-)) and chondrogenic differentiation medium (Diff (+)) for 4 weeks.

3.3. Expression of Chondrogenic Differentiation Marker Genes

To evaluate chondrogenic behavior in 3D silica fabrics in more detail, the expression of chondrogenic differentiation marker genes, *COL1A1*, *COL2A1*, *COL10A1*, *ACAN*, and *SOX9*, was investigated by qRT-PCR (Figure 5). For almost all the genes, differences in expression were preferentially observed between normal and differentiation conditions. Under differentiation condition, the expression of *COL2A1* in atelocollagen and 3D silica fabric culture was superior to that in spheroid culture, but the expression of *ACAN* was the most elevated in spheroid culture. The expression of *SOX9* was the same in all scaffolds. The expression levels of *COL1A1* and *COL10A1* in spheroid culture were superior to those in the other scaffolds, and they were the lowest in 3D silica fabric culture. Chondrogenic differentiation of MSCs in each scaffold was also evaluated by assessing GAG and COL accumulation. These results suggested that 3D silica fabric culture was useful in the development of tissue-engineered constructs, particularly for cartilage formation, and that it is equivalent or superior to atelocollagen gel culture as a commodity scaffold.

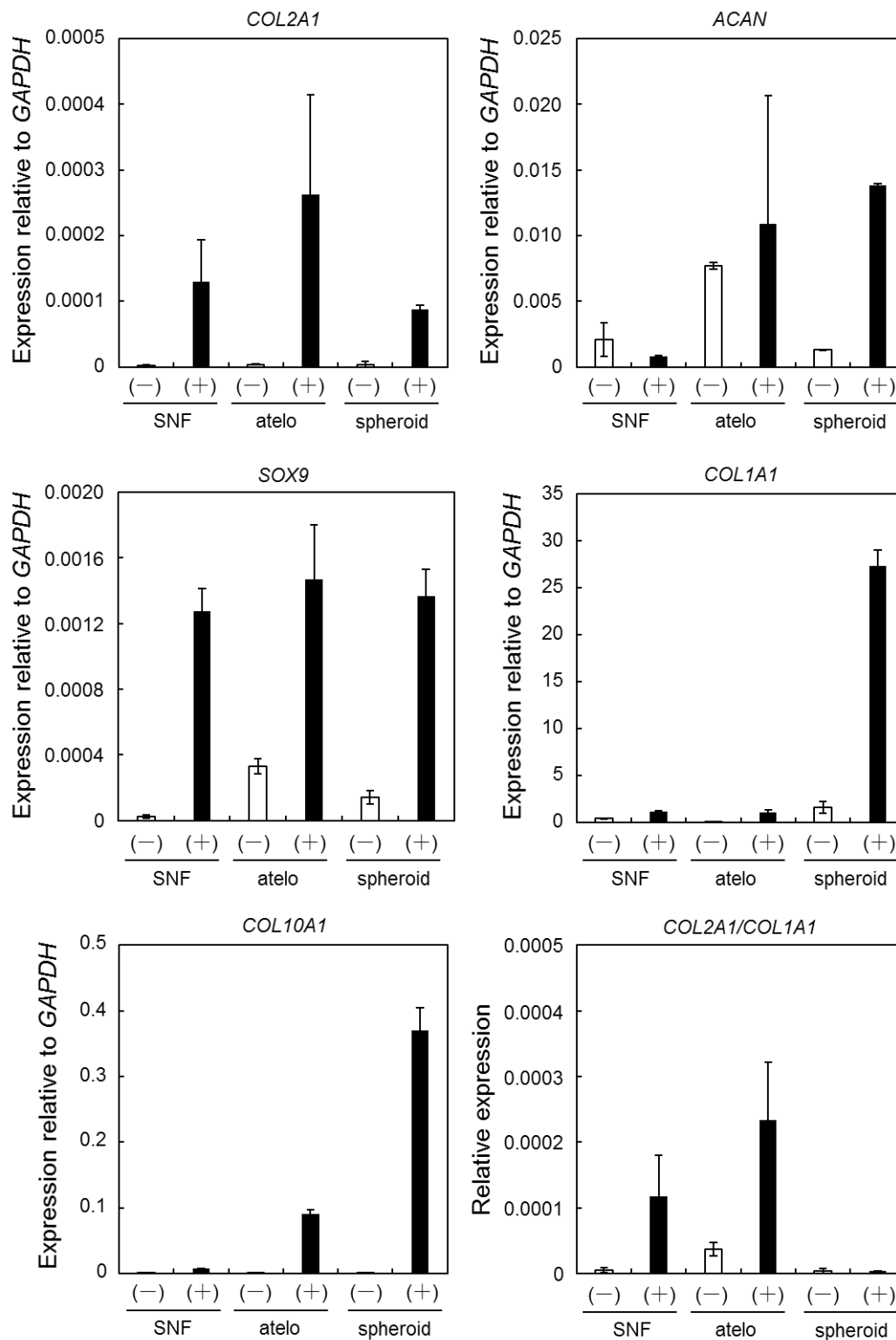


Figure 5. The expression of *COL1A1*, *COL2A1*, *COL10A1*, *ACAN*, and *SOX9* in mesenchymal stem cells (MSCs) cultured on 3D silica fibers in normal medium (Diff (-)) and chondrogenic differentiation medium (Diff (+)). Signal intensity was normalized using that of a control housekeeping gene (human *GAPDH* gene).

4. Discussion

In the present study, chondrogenic differentiation of human bone marrow-derived MSCs in 3D silica fabrics was investigated. For the chondrogenic differentiation of MSCs, we utilized 3D silica fabrics as previously reported, as it is a reasonable scaffold for tissue engineering [34–36,38]. Briefly, 3D silica fabrics were developed via the sol-gel process to create highly interconnected porous microstructures of electrospun fabrics for cell growth. 3D silica fabrics have a high porosity of approximately 95% and an average pore size of 7.6 μm ($n = 5$). The diameter of the fibers constituting the 3D silica fabrics was 704 ± 280 nm ($n = 50$). The random orientation of the silica fibers produced many interconnected pores that may promote cellular infiltration and tissue ingrowth while preventing shrinkage and contraction during cell culture due to the inherent mechanical strength.

The thickness of the MSC layers in the 3D silica fabrics under normal and differentiation conditions was dependent on the culture, and MSCs under normal culture were laminated compared with those in differentiation condition. These results indicate that DNA synthesis under normal condition was promoted in 3D silica fabrics. We have previously demonstrated that fibroblasts cultured in 3D silica fabrics showed remarkable growth rates compared with those in traditional 2D culture [34]. The results in this study suggested that MSCs migrated vertically and proliferated effectively in 3D environments without receiving signals of contact inhibition. Moreover, the MSC layers in silica fabrics under differentiation condition were thicker, which indicated that the cell attachment region in 3D silica fabrics was limited by the accumulation of ECM components, such as aggrecan and collagen. This result also supported the vertical migration of MSCs under chondrogenic condition and formation of 3D cellular layers in 3D silica fabrics.

The number of cells in 3D silica fabrics under differentiation condition stimulated by medium containing chondrogenic factors, TGF- β , ascorbic acid, and dexamethasone was controlled compared with that in normal condition. TGF- β activates TGF- β receptor II on the cell surface and then binds with TGF- β receptor I, inducing the combination of TGF- β receptor I and II into a heteromeric complex and activating the downstream Smad pathway [46]. In addition, TGF- β is known to control the increase in cell number, such as TGF- β , feedback and aggravate the production of ECM proteins, such as fibronectin, aggrecan, and collagen [47–49]. Thus, the number of cells in 3D silica fabrics under differentiation condition is inferior to that under normal condition, which strongly indicates that TGF- β works in 3D silica fabrics without deactivation. These results are highly correlated to the CLSM images.

In chondrogenic differentiation, the accumulation of GAG and COL in 3D silica fabrics was increased compared with that in normal condition. GAG production is one of the key early indicators of a chondrocyte-like phenotype. Native cartilage comprises primarily sulfated GAG chains and type II collagen [50]. Thus, effective accumulation in 3D silica fabrics is a promising result for cartilage tissue engineering.

Finally, we investigated chondrogenic behavior in 3D silica fabrics in detail. *SOX9* is an early-stage marker and a major regulator of chondrogenesis, and it was expressed significantly at the mRNA level in MSCs under differentiation condition in each scaffold. *SOX9* is required for *SOX5* and *SOX6* expression and, together, *SOX5*, *SOX6*, and *SOX9* (the SOX trio) coordinately regulate the expression of several cartilage matrix genes including *ACAN*, *COL2A1*, and *COL1A1* [50]. During endochondral bone formation, *SOX9* expression is downregulated in growth plate chondrocytes as they undergo maturation and begin to express markers of hypertrophy, such as *RUNX2* and *COL10A1* [51]. In articular cartilage, *SOX9* is crucial for the maintenance of the ECM as chondrocyte-specific postnatal deletion of *SOX9* results in reduced matrix proteoglycan content probably as a result of increased *ADAMTS5* expression [52]. Thus, each scaffold in the study is useful for cartilage tissue formation. Moreover, as mentioned above, *ACAN* and *COL1A1* were used as markers of chondrogenesis with *COL1A1* being a marker of fibrocartilage formation. The gene expression of chondrogenic markers *COL2A1*, *ACAN*, and *SOX9* indicates that each scaffold significantly enhanced chondrogenic differentiation of MSCs under differentiation condition. *COL2A1* mRNA expression increased in the order of spheroids,

3D silica fabrics, and atelocollagen gels, and the *COL1A1* and *COL10A1* mRNA expression increased in the order of 3D silica fabrics, atelocollagen gels, and spheroids. These results indicate that MSCs cultured in spheroids promoted the formation of fibrocartilage or hypertrophic cartilage and, as a result, the accumulation of COL in spheroids was greater than that in 3D silica fabrics. Furthermore, *COL10A1* mRNA in atelocollagen gels was overexpressed compared with that in 3D silica fabrics. *COL10A1* is the only known hypertrophic chondrocyte-specific molecular marker. Mutations in *COL10A1* in humans have been associated with Schmid metaphyseal chondrodysplasia. These results support the superiority or equivalence of 3D silica fabric culture under chondrogenic differentiation condition to atelocollagen gels and spheroids, which are commodity scaffolds used as controls.

We have already demonstrated that 3D silica fabrics promoted the osteogenic differentiation of MSCs. In bone-cartilage regeneration, hardness and absorbability of the scaffold are particularly important factors [53,54]. Previously, we concluded that osteogenic differentiation was strongly promoted in 3D silica fabrics because of the high rigidity, porosity, and permeability of the scaffold compared with those of 2D polystyrene dish. Thus, in this report, we supposed that chondrogenic differentiation in 3D silica fabrics was promoted because of these factors.

Commonly, chondrogenic differentiation of MSCs has been investigated by utilizing 2D or 3D scaffolds, such as nano and microfibrillar or porous scaffolds including poly (ϵ -caprolactone) and poly (L-lactide), which have comparable stiffnesses to that of native cartilage [54,55]. Aside from soluble factors, factors affecting chondrogenic differentiation of MSCs are classified into two categories. The first is cell–cell and the second, cell–ECM interactions. The 3D nanofibrillar structures of the silica fabrics share morphological similarities to collagen fibrils and enable favorable biological responses to be promoted for chondrogenic differentiation. Furthermore, the high interconnectivity of 3D silica fabrics allows cells to interact with surrounding cells. The latter factor is the elasticity of substrates. Chondrogenic differentiation of MSCs was strongly affected by elastic substrates and rigid matrices [56,57]. The 3D silica fabrics are highly interconnected network structures and rigid substrates compared with atelocollagen gels. Therefore, these features contributed to the promotion of chondrogenic differentiation in MSCs. Furthermore, atelocollagen gels are animal-derived scaffold and have its shrinking property, so the clinical application is limited. Thus, the application of 3D silica fabrics that replace atelocollagen gels is expected.

On the other hand, the primary goal of cartilage tissue engineering is to regenerate neo-tissues that have similar biomechanical functions as those of native tissue. Chitosan, hyaluronic acid, and collagen provide suitable environments for chondrocyte and matrix deposition. However, the mechanical properties of the engineered tissue are not strong enough to endure physiological loading upon clinical implantation. Ideally, cartilage constructs should show compressive stiffness of 0.5–6.0 MPa [58]. Several studies on engineered cartilage constructs have reported mechanical properties at the kPa range, which are not nearly strong enough for physiological loading. Indeed, we have demonstrated that the compressive strength of 3D silica fabrics is 0.2 MPa, which is not stiff enough for use in tissue repair. Since the seeded cells are able to produce ample biological matrix, reasonable scaffold designs should contain more optimized geometry, thereby rendering mechanical properties closer to that of native tissues. The present study shows the extent to which cells seeded on large pore constructs can produce biochemical components while maintaining strong mechanical properties. Even after the scaffolds biodegrade at a later time point, this, theoretically, will allow engineered tissues to withstand high loads immediately after implantation.

We previously demonstrated the high permeability of 3D silica fabrics in culture inserts, which were used for biological investigation of heterotypic cell–cell interaction and co-culture [34]. In fact, it is also suggested that paracrine factors secreted from non-parenchymal cells placed at the top insert were permeated and had enhanced hepatocyte functions in co-culture systems. Therefore, the excellent permeability of 3D silica fabrics seems to be effective for chondrogenesis of stem cells therein. While we only examined chondrogenic differentiation, 3D silica fabrics can be a material that

finds advantages in terms of both strength and differentiation, although the performance is inferior to those of spheroids and atelocollagen as highly functional scaffolds.

5. Conclusions

In this study, chondrogenic differentiation of bone marrow-derived MSCs in 3D silica fabrics was investigated. MSCs under chondrogenic differentiation condition migrated and proliferated inside the 3D silica fabrics. Compared with conventional spheroid and atelocollagen gel culture, the 3D silica fabrics strongly promoted the chondrogenic differentiation of MSCs. These results suggested that 3D silica fabrics are promising scaffolds for the regeneration of cartilage defects using MSCs. This bio-glass based scaffold composed of oxides including SiO₂, Na₂O, CaO, and P₂O₅ has been demonstrated as clinical application use such as bone and cartilage tissue regeneration [59,60] so the application of designed 3D silica fabrics will be increasing in tissue engineering.

Author Contributions: Conceptualization, H.O.; Methodology, K.S. and M.K.; Writing—original draft preparation, S.I.; Writing—review and editing, K.I.; Supervision, H.O. and M.H.

Funding: This research received no external funding.

Conflicts of Interest: The authors declare no conflict of interest.

References

1. Clar, C.; Cummins, E.; McIntyre, L.; Thomas, S.; Bain, L.; Jobanputra, P.; Waugh, N. Clinical and cost-effectiveness of autologous chondrocyte implantation for cartilage defects in knee joints: systematic review and economic evaluation. *Health Technol. Assess.* **2005**, *9*, 1–82. [[CrossRef](#)]
2. Knutsen, G.; Engebretsen, L.; Ludvigsen, T.C.; Drogset, J.O.; Grøntvedt, T.; Solheim, E.; Strand, T.; Roberts, S.; Isaksen, V.; Johansen, O. Autologous chondrocyte implantation compared with microfracture in the knee. A randomized trial. *J. Bone Joint Surg. Am.* **2004**, *86*, 455–464. [[CrossRef](#)] [[PubMed](#)]
3. Robert, B.; Dzioba, M.D. The classification and treatment of acute articular cartilage lesions. *Arthroscopy* **1988**, *4*, 72–80. [[CrossRef](#)]
4. Hutmacher, D.W. Scaffolds in tissue engineering bone and cartilage. *Biomaterials* **2000**, *21*, 2529–2543. [[CrossRef](#)]
5. Sherwood, J.K.; Riley, S.L.; Palazzolo, R.; Brown, S.C.; Monkhouse, D.C.; Coates, M.; Griffith, L.G.; Landeen, L.K.; Ratcliffe, A. A three-dimensional osteochondral composite scaffold for articular cartilage repair. *Biomaterials* **2002**, *23*, 4739–4751. [[CrossRef](#)]
6. Jiang, C.C.; Chiang, H.; Liao, C.J.; Lin, Y.J.; Kuo, T.F.; Shieh, C.S.; Huang, Y.Y.; Tuan, R.S. Repair of porcine articular cartilage defect with a biphasic osteochondral composite. *J. Orthop. Res.* **2007**, *25*, 1277–1290. [[CrossRef](#)] [[PubMed](#)]
7. Hangody, L.; Füles, P. Autologous osteochondral mosaicplasty for the treatment of full-thickness defects of weight-bearing joints. *J. Bone Joint Surg. Am.* **2003**, *85*, 25–32. [[CrossRef](#)] [[PubMed](#)]
8. Barry, F.P.; Murphy, J.M. Mesenchymal stem cells: clinical applications and biological characterization. *Int. J. Biochem. Cell Biol.* **2004**, *36*, 568–584. [[CrossRef](#)] [[PubMed](#)]
9. Wakitani, S.; Imoto, K.; Yamamoto, T.; Saito, M.; Murata, N.; Yoneda, M. Human autologous culture expanded bone marrow mesenchymal cell transplantation for repair of cartilage defects in osteoarthritic knees. *Osteoarthr. Cartil.* **2002**, *10*, 199–206. [[CrossRef](#)] [[PubMed](#)]
10. Caplan, A.I. Adult mesenchymal stem cells for tissue engineering versus regenerative medicine. *J. Cell. Physiol.* **2007**, *213*, 341–347. [[CrossRef](#)] [[PubMed](#)]
11. Pittenger, M.F.; Mackay, A.M.; Beck, S.C.; Jaiswal, R.K.; Douglas, R.; Mosca, J.D.; Moorman, M.A.; Simonetti, D.W.; Craig, S.; Marshak, D.R. Multilineage potential of adult human mesenchymal stem cells. *Science* **1999**, *2*, 143–147. [[CrossRef](#)]
12. Mani, S.A.; Guo, W.; Liao, M.J.; Eaton, E.N.; Ayyanan, A.; Zhou, A.Y.; Brooks, M.; Reinhard, F.; Zhang, C.C.; Shipitsin, M.; et al. The epithelial-mesenchymal transition generates cells with properties of stem cells. *Cell* **2008**, *133*, 704–715. [[CrossRef](#)] [[PubMed](#)]

13. Jiang, Y.; Jahagirdar, B.N.; Reinhardt, R.L.; Schwartz, R.E.; Keene, C.D.; Ortiz-Gonzalez, X.R.; Reyes, M.; Lenvik, T.; Lund, T.; Blackstad, M.; Du, J.; Aldrich, S.; Lisberg, A.; Low, W.C.; Largaespada, D.A.; Verfaillie, C.M. Pluripotency of mesenchymal stem cells derived from adult marrow. *Nature* **2002**, *418*, 41–49. [[CrossRef](#)] [[PubMed](#)]
14. C Murphy, C.A.; Costa, J.B.; Silva-Correia, J.; Oliveira, J.M.; Reis, R.L.; Collins, M.N. Biopolymers and polymers in the search of alternative treatments for meniscal regeneration: State of the art and future trends. *Applied Materials Today* **2018**, *12*, 51–71. [[CrossRef](#)]
15. Hung, A.H.; Farrell, M.J.; Mauck, R.L. Mechanics and mechanobiology of mesenchymal stem cell-based engineered cartilage. *J. Biomech.* **2010**, *43*, 128–136. [[CrossRef](#)] [[PubMed](#)]
16. Yamaoka, H.; Tanaka, Y.; Nishizawa, S.; Asawa, Y.; Hoshi, K. The application of atelocollagen gel in combination with porous scaffolds for cartilage tissue engineering and its suitable conditions. *J. Bio. Mat. Res. A* **2009**, *93*, 123–132. [[CrossRef](#)] [[PubMed](#)]
17. Charriere, G.; Bejot, M.; Schnitzler, L.; Ville, G.; Hartmann, D.J. Reactions to a bovine collagen implant. Clinical and immunologic study in 705 patients. *J. Am. Acad. Dermatol* **1989**, *21*, 1203–1208. [[CrossRef](#)]
18. Shepherd, D.E.; Seedhom, B.B. The ‘instantaneous’ compressive modulus of human articular cartilage in joints of the lower limb. *Rheumatology* **1998**, *38*, 124–132. [[CrossRef](#)]
19. Hennig, T.; Lorenz, H.; Thiel, A.; Goetzke, K.; Dickhut, A.; Geiger, F.; Richter, W. Reduced chondrogenic potential of adipose tissue derived stromal cells correlates with an altered TGF β receptor and BMP profile and is overcome by BMP-6. *J. Cell. Physiol.* **2007**, *211*, 682–691. [[CrossRef](#)] [[PubMed](#)]
20. Huang, G.S.; Hsieh, P.S.; Tseng, C.S.; Hsu, S.H. The substrate-dependent regeneration capacity of mesenchymal stem cell spheroids derived on various biomaterial surfaces. *Biomater. Sci.* **2014**, *2*, 1652–1660. [[CrossRef](#)]
21. Bosnakovski, D.; Mizuno, M.; Kim, G.; Takagi, S.; Okumura, M.; Fujinaga, T. Chondrogenic differentiation of bovine bone marrow mesenchymal stem cells (MSCs) in different hydrogels: influence of collagen type II extracellular matrix on MSC chondrogenesis. *Biotechnol. Bioeng.* **2006**, *93*, 1152–1163. [[CrossRef](#)] [[PubMed](#)]
22. Meng, Q.; Man, Z.; Dai, L.; Huang, H.; Zhang, X.; Hu, X.; Shao, Z.; Zhu, J.; Zhang, J.; Fu, X.; Duan, X.; Ao, Y. A composite scaffold of MSC affinity peptide-modified demineralized bone matrix particles and chitosan hydrogel for cartilage regeneration. *Sci. Rep.* **2015**, *5*, 17802. [[CrossRef](#)] [[PubMed](#)]
23. Wang, Y.; Kim, U.J.; Blasioli, D.J.; Kim, H.J.; Kaplan, D.L. In vitro cartilage tissue engineering with 3D porous aqueous-derived silk scaffolds and mesenchymal stem cells. *Biomaterials* **2005**, *26*, 7082–7094. [[CrossRef](#)] [[PubMed](#)]
24. Karkhaneh, A.; Naghizadeh, Z.; Shokrgozar, M.S.; Bonakdar, S. Evaluation of the chondrogenic differentiation of mesenchymal stem cells on hybrid biomimetic scaffolds. *J. Appl. Polym. Sci.* **2014**, *131*, 40635. [[CrossRef](#)]
25. Li, W.J.; Tuli, R.; Okafor, C.; Derfoul, A.; Danielson, K.G.; Hall, D.J.; Tuan, R.S. A three-dimensional nanofibrous scaffold for cartilage tissue engineering using human mesenchymal stem cells. *Biomaterials* **2005**, *26*, 599–609. [[CrossRef](#)] [[PubMed](#)]
26. Souness, A.; Zamboni, F.; Walker, G.M.; Collins, M.N. Influence of scaffold design on 3D printed cell constructs. *J. Biomed. Mater. Res. B Appl. Biomater.* **2018**, *106*, 533–545. [[CrossRef](#)] [[PubMed](#)]
27. Li, W.J.; Tuli, R.; Huang, X.; Laquerriere, P.; Tuan, R.S. Multilineage differentiation of human mesenchymal stem cells in a three-dimensional nanofibrous scaffold. *Biomaterials* **2005**, *26*, 5158–5166. [[CrossRef](#)] [[PubMed](#)]
28. Cao, Y.; Li, D.; Shang, C.; Yang, S.T.; Wang, J.; Wang, X. Three-dimensional culture of human mesenchymal stem cells in a polyethylene terephthalate matrix. *Biomed. Mater.* **2010**, *5*, 065013. [[CrossRef](#)] [[PubMed](#)]
29. Ardeshirylajimi, A.; Mossahebi-Mohammadi, M.; Vakilian, S.; Langroudi, L.; Seyedjafari, E.; Atashi, A.; Soleimani, M. Comparison of osteogenic differentiation potential of human adult stem cells loaded on bioceramic-coated electrospun poly (L-lactide) nanofibres. *Cell Prolif.* **2015**, *48*, 47. [[CrossRef](#)] [[PubMed](#)]
30. Pournaqi, F.; Ghiaee, A.; Vakilian, S.; Ardeshirylajimi, A. Improved proliferation and osteogenic differentiation of mesenchymal stem cells on polyaniline composited by polyethersulfone nanofibers. *Biologicals* **2017**, *45*, 78–84. [[CrossRef](#)] [[PubMed](#)]
31. Shafiee, A.; Soleimani, M.; Chamheidari, G.A.; Seyedjafari, E.; Dodel, M.; Atashi, A.; Gheisari, Y. Electrospun nanofiber-based regeneration of cartilage enhanced by mesenchymal stem cells. *J. Biomed. Mater. Res. A* **2011**, *99*, 467–478. [[CrossRef](#)] [[PubMed](#)]

32. Shin, H.J.; Lee, C.H.; Cho, I.H.; Kim, Y.J.; Lee, Y.J.; Kim, I.A.; Park, K.D.; Yui, N.; Shin, J.W. Electrospun PLGA nanofiber scaffolds for articular cartilage reconstruction: mechanical stability, degradation and cellular responses under mechanical stimulation in vitro. *J. Biomater. Sci. Polym. Ed.* **2006**, *17*, 103–119. [[CrossRef](#)] [[PubMed](#)]
33. Yamaguchi, T.; Sakai, S.; Watanabe, R.; Tarao, T.; Kawakami, K. Heat treatment of electrospun silicate fiber substrates enhances cellular adhesion and proliferation. *J. Biosci. Bioengin.* **2010**, *109*, 304–306. [[CrossRef](#)] [[PubMed](#)]
34. Yamaguchi, Y.; Deng, D.; Sato, Y.; Hou, Y.T.; Watanabe, R.; Sasaki, K.; Kawabe, M.; Hirano, E.; Morinaga, T. Silicate fiber-based 3D cell culture system for anticancer drug screening. *Anticancer Res.* **2013**, *33*, 5301–5309. [[PubMed](#)]
35. Otsuka, H.; Sasaki, K.; Okimura, S.; Nagamura, M.; Watanabe, R.; Kawabe, M. Contribution of fibroblasts cultured on 3D silica nonwoven fabrics to cocultured hepatocytes function. *Chem. Lett.* **2014**, *43*, 343–345. [[CrossRef](#)]
36. Kascholke, C.; Hendrikx, S.; Flath, T.; Kuzmenka, D.; Dörfler, H.M.; Schumann, D.; Gressenbuch, M.; Schulze, F.P.; Schulz-Siegmund, M.; Hacker, M.C. Biodegradable and adjustable sol-gel glass based hybrid scaffolds from multi-armed oligomeric building blocks. *Acta Biomater.* **2017**, *63*, 336. [[CrossRef](#)] [[PubMed](#)]
37. Mori, T.; Kiyono, T.; Imabayashi, H.; Takeda, Y.; Tsuchiya, K.; Miyoshi, S.; Makino, H.; Matsumoto, K.; Saito, H.; Ogawa, S.; Sakamoto, M.; Hata, J.; Umezawa, A. Combination of hTERT and *bmi-1*, E6, or E7 induces prolongation of the life span of bone marrow stromal cells from an elderly donor without affecting their neurogenic potential. *Mol. Cell. Biol.* **2005**, *25*, 5183–5195. [[CrossRef](#)] [[PubMed](#)]
38. Mueller, S.M.; Shortkro, S.; Schneider, T.O.; Breinan, H.A.; Yannas, L.V.; Spector, T.O. Meniscus cells seeded in type I and type II collagen–GAG matrices in vitro. *Biomaterials* **1999**, *20*, 701–709. [[CrossRef](#)]
39. Bahney, C.S.; Hsu, S.W.; Yoo, J.U.; West, J.L.; Johnstone, B. A bioresponsive hydrogel tuned to chondrogenesis of human mesenchymal stem cells. *FASEB* **2011**, *25*, 1486–1496. [[CrossRef](#)] [[PubMed](#)]
40. Woessner, J.F. The determination of hydroxyproline in tissue and protein samples containing small proportions of this imino acid. *Arch. Biochem. Biophys.* **1961**, *93*, 440–447. [[CrossRef](#)]
41. Yamashita, A.; Morioka, M.; Yahara, Y.; Okada, M.; Kobayashi, T.; Kuriyama, S.; Matsuda, S.; Tsumaki, N. Generation of scaffoldless hyaline cartilaginous tissue from human iPSCs. *Stem Cell Reports* **2015**, *4*, 404–418. [[CrossRef](#)] [[PubMed](#)]
42. Chung, C.; Burdick, J.A. Influence of three-dimensional hyaluronic acid microenvironments on mesenchymal stem cell chondrogenesis. *Tissue Eng. Part A* **2009**, *15*, 243–254. [[CrossRef](#)] [[PubMed](#)]
43. Xu, J.; Wang, W.; Ludeman, M.; Cheng, K.; Hayami, T.; Lotz, J.C.; Kapila, S. Chondrogenic Differentiation of Human Mesenchymal Stem Cells in Three-Dimensional Alginate Gels. *Tissue Eng. Part A* **2008**, *14*, 667–680. [[CrossRef](#)] [[PubMed](#)]
44. Ko, C.Y.; Yang, C.Y.; Yang, S.R.; Ku, K.L.; Tsao, C.K.; Chuang, D.C.C.; Chu, I.M.; Cheng, M.H. Cartilage formation through alterations of amphiphilicity of poly(ethylene glycol)–poly(caprolactone) copolymer hydrogels. *RSC Adv.* **2013**, *3*, 25769–25779. [[CrossRef](#)]
45. Lin, H.; Cheng, A.W.M.; Alexander, P.G.; Beck, A.M.; Tuan, R.S. Cartilage tissue engineering application of injectable gelatin hydrogel with in situ visible-light-activated gelation capability in both air and aqueous solution. *Tissue Eng. Part A* **2014**, *20*, 2402–2411. [[CrossRef](#)] [[PubMed](#)]
46. Heldin, C.H.; Miyazono, K.; ten Dijke, P. TGF- β signalling from cell membrane to nucleus through SMAD proteins. *Nature* **1997**, *390*, 465–471. [[CrossRef](#)] [[PubMed](#)]
47. Huang, S.S.; Huang, J.S. TGF- β control of cell proliferation. *J. Cell Biochem.* **2005**, *96*, 447–462. [[CrossRef](#)] [[PubMed](#)]
48. Patil, A.S.; Sable, R.B.; Kothari, R.M. An update on transforming growth factor- β (TGF- β): sources, types, functions and clinical applicability for cartilage/bone healing. *J. Cell. Physiol.* **2011**, *226*, 3094–3103. [[CrossRef](#)] [[PubMed](#)]
49. Richardson, S.M.; Kalamegam, G.; Pushparaj, P.N.; Matta, C.; Memic, A.; Khademhosseini, A.; Mobasheri, R.; Poletti, F.L.; Hoyland, J.A.; Mobasheri, A. Mesenchymal stem cells in regenerative medicine: Focus on articular cartilage and intervertebral disc regeneration. *Methods* **2016**, *99*, 69–80. [[CrossRef](#)] [[PubMed](#)]
50. Martinez-Sanchez, A.; Dudek, K.A.; Murphy, C.L. Regulation of human chondrocyte function through direct inhibition of cartilage master regulator SOX9 by microRNA-145 (miRNA-145). *J. Biol. Chem.* **2012**, *287*, 916–924. [[CrossRef](#)] [[PubMed](#)]

51. Dy, P.; Wang, W.; Bhattaram, P.; Wang, Q.; Wang, L.; Ballock, R.T.; Lefebvre, V. Sox9 directs hypertrophic maturation and blocks osteoblast differentiation of growth plate chondrocytes. *Dev. Cell* **2012**, *22*, 597–609. [[CrossRef](#)]
52. Tsirimonaki, E.; Fedonidis, C.; Pneumaticos, S.G.; Tragas, A.A.; Michalopoulos, I.; Mangoura, D. PKC ϵ signalling activates ERK1/2, and regulates aggrecan, ADAMTS5, and miR377 gene expression in human nucleus pulposus cells. *PLoS One* **2013**, *8*, e82045. [[CrossRef](#)] [[PubMed](#)]
53. Liao, H.T.; Chen, C.T.; Chen, J.P. Osteogenic differentiation and ectopic bone formation of canine bone marrow-derived mesenchymal stem cells in injectable thermo-responsive polymer hydrogel. *Tissue Eng. Part C Methods* **2011**, *17*, 1139–1149. [[CrossRef](#)] [[PubMed](#)]
54. Visser, J.; Melchels, F.P.; Jeon, J.E.; van Bussel, E.M.; Kimpton, L.S.; Byrne, H.M.; Dhert, W.J.; Dalton, P.D.; Huttmacher, D.W.; Malda, J. Reinforcement of hydrogels using three-dimensionally printed microfibrils. *Nat. Commun.* **2015**, *6*, 6933. [[CrossRef](#)] [[PubMed](#)]
55. Garrigues, N.W.; Little, D.; Sanchez-Adams, J.; Ruch, D.S.; Guilak, F. Electrospun cartilage-derived matrix scaffolds for cartilage tissue engineering. *J. Biomed. Mater. Res. A* **2014**, *102*, 3998–4008. [[CrossRef](#)] [[PubMed](#)]
56. Shariati, S.R.P.; Moeinzadeh, S.; Jabbari, E. Nanofiber Based Matrices for Chondrogenic Differentiation of Stem Cells. *J. Nanosci. Nanotechnol.* **2016**, *16*, 8966–8977. [[CrossRef](#)]
57. Schlichting, K.; Schell, H.; Kleemann, R.U.; Schill, A.; Weiler, A.; Duda, G.N.; Epari, D.R. Influence of scaffold stiffness on subchondral bone and subsequent cartilage regeneration in an ovine model of osteochondral defect healing. *Am. J. Sports Med.* **2008**, *36*, 2379–2391. [[CrossRef](#)] [[PubMed](#)]
58. Li, X.; Chen, S.; Li, J.; Wang, X.; Zhang, J.; Kawazoe, N.; Chen, G. 3D culture of chondrocytes in gelatin hydrogels with different stiffness. *Polymers* **2016**, *8*, 269. [[CrossRef](#)]
59. Zhou, M.; Yu, D. Cartilage tissue engineering using PHBV and PHBV/Bioglass scaffolds. *Mol. Med. Rep.* **2014**, *10*, 508–514. [[CrossRef](#)] [[PubMed](#)]
60. Crovace, M.C.; Souza, M.T.; Chinaglia, C.R.; Peitl, O.; Zanotto, E.D. Biosilicate®—A multipurpose, highly bioactive glass-ceramic. *In vitro, in vivo* and clinical trials. *J. Non-Cryst. Solids* **2016**, *432*, 90–110. [[CrossRef](#)]



© 2018 by the authors. Licensee MDPI, Basel, Switzerland. This article is an open access article distributed under the terms and conditions of the Creative Commons Attribution (CC BY) license (<http://creativecommons.org/licenses/by/4.0/>).